ESPI-system with active in-line digital phase stabilization

Heinz Helmers, Matthias Bischoff and Lars Ehlkes

Carl-von-Ossietzky Universität Oldenburg, FB Physik, Applied Optics
PF 2503, D-26111 Oldenburg

heinz.helmers@uni-oldenburg.de

1 Introduction

In an electronic speckle pattern interferometer (ESPI) the light intensity I in the speckle interferogram is given by:

$$(1) \qquad I(x,y,t) = I_b(x,y) + I_m(x,y)\cos\left(\varphi_R(x,y) - \varphi_O(x,y) - \Delta\varphi_O(x,y,t)\right)$$

$I_b = I_R + I_O$ is the background intensity, I_R and I_O are the intensities of the reference wave and the speckled object wave, φ_R and φ_O are their phases, $\Delta\varphi_O$ is the phase change of the object wave due to object deformation, and $I_m = 2\sqrt{I_R\, I_O}$ is the modulation. All these quantities depend on the spatial coordinates (x,y), additionally $\Delta\varphi_O$ and therefore I too depend on the time t (the minor time dependence of I_O and φ_O caused by speckle decorrelation is ignored). The aim of ESPI is to measure the temporal course of $I(x,y,t)$ and to calculate from that the course of $\Delta\varphi_O$ using temporal and spatial phase shifting techniques /1, 2/.

In praxis these measurements are frequently disturbed by random phase fluctuations. We will confine ourselves to those fluctuations that are caused by pressure and temperature fluctuations in optical fibres, large scale temperature fluctuations in regions where the light is not guided by fibres, mechanical vibrations, and drifts in components. All these effects result in global phase fluctuations $\varphi_g(t)$ that are constant over the field of measurement but vary in time. The phase φ in Eq. (1) is then given by $\varphi = \varphi_R - \varphi_O - \Delta\varphi_O + \varphi_g$.

In /3/ we presented a first version of an ESPI-system with integrated active phase stabilization. The system requires no additional optical components and stabilizes the phase φ at a point P in the field of measurement. By this stabilization $\varphi_g(t)$ has no longer any influence on the measurement of $\Delta\varphi_O(x,y,t)$, for which P is now the reference point. Fig. 1 shows the principal set-up of the system. The light of a laser diode LD (SDL 5421-G1, 150 mW @ 835 nm) passes through an optical isolator OI (inverse isolation 37 dB) and a half-wave-plate HW and is coupled into a single-mode polarization maintaining fibre (Scotch 3M HB4611) with a microscopic objective MO. A fibre coupler FC splits the light into an object beam O and a reference beam R. Both beams pass through fibres of about 30 m length, of which some 26 metres are wound on piezoelectric cylinders PZ_R and PZ_O of about 55 mm diameter. The object illuminated by O is imaged by an objective OB with aperture A_{OB} onto the target of a CCD camera (Sony XC 75 CE), where its speckled image is superimposed with R, which is directed onto the target by a beam splitter BS.

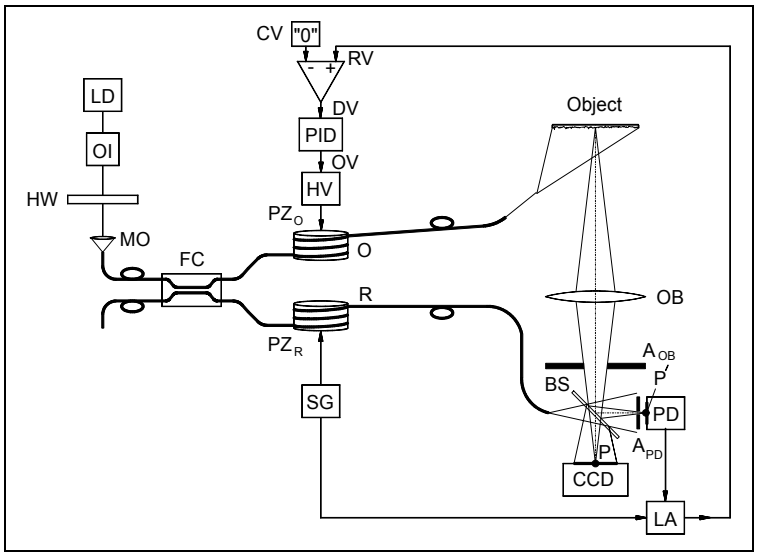

Fig. 1: Set-up of the ESPI-system with integrated active phase stabilization

The phase stabilization is achieved by a synthetic heterodyne technique for which the phase of the reference wave is modulated with angular frequency ω. This is realized by a sinusoidal variation of the optical path of R by changing the diameter of PZ_R with a suitable modulation voltage from a signal generator SG. With α being the amplitude of the phase modulation, the phase φ is now given by:

$$\varphi = \varphi_R - \varphi_O - \Delta\varphi_O + \varphi_g + \alpha\sin(\omega t) := \Phi + \alpha\sin(\omega t) \tag{2}$$

Inserting Eq. (2) in Eq. (1) and expanding $\cos(\alpha\sin(\omega t))$ and $\sin(\alpha\sin(\omega t))$ in Fourier series gives the intensity I_{PD}, which is measured by the photo detector PD at the point P', where φ is the same as at the point P:

$$I_{PD} = I_b + I_m \left\{ \begin{array}{l} \cos(\Phi)\left(J_0(\alpha) + 2\sum_{j=1}^{\infty} J_{2j}(\alpha)\cos(2j\omega t)\right) \\ -\sin(\Phi)\left(2\sum_{j=1}^{\infty} J_{2j-1}(\alpha)\sin((2j-1)\omega t)\right) \end{array} \right\} \tag{3}$$

with J_j being the Bessel functions of first kind and order j. Eq. (3) shows, that the output signal of PD includes signal components at frequencies $j\omega$. This signal is fed into a lock-in amplifier LA, whose reference signal is the modulation voltage of the signal generator. The output signal of LA is the regulated value RV of a PID-controller. Finally, the output signal of the PID-controller is connected to a high voltage amplifier HV which drives the second piezoelectric cylinder PZ_O. PZ_O is the control device in the feedback control system, it can change the phase φ_O in the range of ± 780 π. The command value CV of the PID-controller is set to „0“. Therefore, in order to achieve a deviation value DV of „0“, the output signal of LA has to be „0“ too. This is the case, if I_{PD} does not include signal components at the modulation frequency ω. Following Eq. (3), this requires $\sin(\Phi) = 0$. Therefore, the PID-controller stabilizes the phase at P' (and P) to a value of $\Phi = 0$ (or integer multiples of π).

In praxis, the integration time τ of LA and the dead time of the PID-controller limit the frequency ν of phase fluctuations $\varphi_g(t)$, which can be sufficiently compensated by the system. In order to achieve a high cut-off frequency for ν, a high modulation frequency ω is needed. Beyond this, the amplitude α of the phase modulation should be low, so that the modulation in the recorded speckle interferogram is not reduced too much. If the exposure time of the CCD-camera is large compared to $2\pi/\omega$, the exposure can be calculated from Eq. (1) and (2) and is proportional to the temporal mean of the intensity I_{CCD} at the CCD-target:

$$(4) \qquad \left\langle I_{\mathrm{CCD}} \right\rangle_t \sim \frac{\omega}{2\pi} f \int_0^{2\pi/\omega} I \, \mathrm{d}t = I_b + I_m J_0(\alpha)\cos(\Phi)$$

Thus, the modulation in the recorded speckle interferogram is reduced by a factor $J_0(\alpha)$. Both conditions (high ω and low α) require a high cut-off frequency and a high signal to noise ratio of the photo detector PD (Hamamatsu photodiode S5973-01 with low noise amplifier; NEP ≈ 8 fW/(Hz)$^{1/2}$ @ 835 nm). Because the amplification-bandwidth product of this detector is limited, a low amplification factor is required in order to achieve a high ω. This can only be achieved, if enough light falls onto the detector, which requires enlarging the aperture A_{PD}. On the other hand, the detector then no longer measures the intensity at a point P', but integrates the intensity over its aperture of diameter D. This leads to an incoherent addition of the intensity of n speckles in the speckle interferogram with randomly distributed intensities I and phases φ. Nevertheless, all time dependent phase variations in Eq. (2) still yield a sufficient modulation in the detector signal, as long as $\Delta\varphi_O$ is nearly the same for all n speckles within the detectors aperture A_{PD}. This is guaranteed if the object deformation gradients are not too large.

In /3/, we justified this principal behaviour of the control system with a heuristic model and confirmed it by computer simulations. The aim of this paper is to replace the heuristic model by an analytical description, which is based on a paper of Lehmann /4/. We will show analytically and experimentally that under the conditions mentioned above the modulation in the detector signal is not only detectable, but increases with $\sqrt{n}$. Beyond this, we will report on some improvements of the ESPI-system with active phase stabilization.

2 Theory

Let us first consider a *speckle pattern* with intensity $I_O(x,y)$, in which the intensity is integrated over an aperture A_{PD} of diameter D of a photo detector. For the calculation of the statistical properties of the integrated intensity I_{PD}, Goodman introduced a box-car approximation /5/, where the detector area is divided into n sub areas of equal size and I_{PD} is given by:

$$(5) \qquad I_{\mathrm{PD}} = \frac{1}{n} \sum_{k=1}^{n} I_k$$

It is assumed, that a) every sub area covers just one speckle with intensity I_k, b) within each sub area I_k = const, c) the I_k are statistically independent, and d) the expected values $\langle I_k \rangle$ are equal for all sub areas. Under these assumptions the density function $p(I_{PD})$ can be calculated from the well known density function $p(I_k)$ of the speckle intensity and its characteristic function.

In order to calculate the statistical quantities of the integrated intensity in a *speckle interferogram*, Lehmann followed the approach of Goodman for a *speckle pattern* /4/. Both authors use the normalization factor (1/*n*) in Eq. (5). If I_{PD} is measured with a detector of small dynamic range (e.g. a 8-Bit CCD-camera with a dynamic range of approx. 48 dB), then it is appropriate to reduce the intensity I_k in the single speckles by a factor 1/*n* if *n* speckles are integrated in order to avoid overloading of the detector. If, on the other hand, a detector with high dynamic range is used (like a photodiode with a dynamic range of 100 dB – 120 dB), this intensity reduction or normalization is not necessary. Therefore, for the integrated intensity in the speckle interferogram we write:

$$(6) \qquad I_{\mathrm{PD}} = \sum_{k=1}^{n} I_k = \sum_{k=1}^{n} \left(I_{b,k}(x,y) + I_{m,k}(x,y) \cos \varphi_k(x,y,t) \right)$$

where the I_k are now given by Eq. (1). Eq. (6) may be written in the form of a usual interferogram equation $I_{\mathrm{PD}} = I_B + I_M \cos(\Theta)$ with

$$(7) \qquad I_B = \sum_{k=1}^{n} I_{b,k}(x,y) \qquad \text{and} \qquad I_M \cos\Theta = \sum_{k=1}^{n} I_{m,k}(x,y) \cos\varphi_k(x,y,t)$$

We are now interested in the expected values of the background intensity, $\langle I_B \rangle$, and the modulation, $\langle I_M \rangle$, as a function of *n*. $\langle I_B \rangle$ may directly be calculated from Eq. (7):

$$(8) \qquad \langle I_B \rangle = \left\langle \sum_{k=1}^{n} I_{b,k} \right\rangle = \sum_{k=1}^{n} \left\langle \left(I_{O,k} + I_R \right) \right\rangle = n \left(\langle I_{O,k} \rangle + I_R \right)$$

with $I_{O,k}$ being the intensity of the object wave in speckle *k*. As expected, $\langle I_B \rangle$ increases linearly with *n*.

For the calculation of $\langle I_M \rangle$ the density function $p(I_M)$ is required. Following the calculations of Lehmann /4/ we find:

$$(9) \qquad p(I_M) = \frac{1}{2nI_R \langle I_{O,k} \rangle} I_M \, \mathrm{e}^{-\frac{I_M^2}{\langle I_{O,k} \rangle 4nI_R}} \qquad \text{and from that} \quad \langle I_M \rangle = \sqrt{n} \sqrt{\pi \langle I_{O,k} \rangle I_R}$$

This result is intuitively surprising because it states that under the mentioned assumptions the expected value of the modulation increases with $\sqrt{n}$. Therefore, in order to confirm Eq. (9), experiments and computer simulations were carried out.

3 Experiment and Results

The measurement of the probability density function and the expected value of the modulation I_M as a function of the number *n* of speckles within the detectors aperture was carried out in a Michelson-interferometer, in which one mirror was replaced by a rough surface. Some of the light scattered by the surface reached the target of a CCD-camera (SONY XC-75CE) as object wave, where is was superimposed with a plane reference wave. 100 speckle interferograms of size 512 × 512 pixel were recorded within 40 s, while the phase φ_R of the reference wave was increased linearly by approx. 5 π by moving the mirror in the reference arm of the

interferometer. The recorded speckle interferograms were divided into segments with $l \times l$ pixel, each covering $n \approx l \times l / 20.25$ speckles, with 20.25 pixel being the mean area of a speckle. For a certain value of n, the grey values of the pixels within each segment were added and tracked through the 100 interferograms. So we got a function proportional to I_{PD}, from which the modulation I_M could be determined. The histogram of I_M is a good approximation for $p(I_M)$, as well as the mean of I_M over all segments is a good approximation for $\langle I_M \rangle$, because both quantities stem from a large number N of segments: $N(n) \approx 512^2/(n \times 20.25)$.

Fig. 2 shows the experimental results and the theoretical curves for $p(I_M)$ (Eq. (9) left) for $n = 5$ and $n = 10$ speckles within the aperture. Both set of curves demonstrate good agreement between the experimental data and the theoretical predictions. Fig. 3 shows the experimental data and the theoretical curve for $\langle I_M \rangle$ as a function of n (Eq. (9) right). Also included are the results of a computer simulation, which was carried out with a method analogue to that described in /3/. Because $\langle I_M \rangle \sim \sqrt{n}$, a straight line with slope ½ is expected in a double logarithmic diagram. The computer simulation shows a very good agreement with the theoretical curve for all n (both curves can be hardly distinguished), and the experimental data are in reasonable agreement with the theoretical predictions. So we can conclude, that under the mentioned conditions the mean of the modulation in the signal of the photo detector PD increases with $\sqrt{n}$. Therefore, its aperture A_{PD} can be widely opened. Although through this $\langle I_B \rangle$ also increases linearly with n, this doesn't affect the detection of the modulation as long as the dynamic range of the detector is high enough.

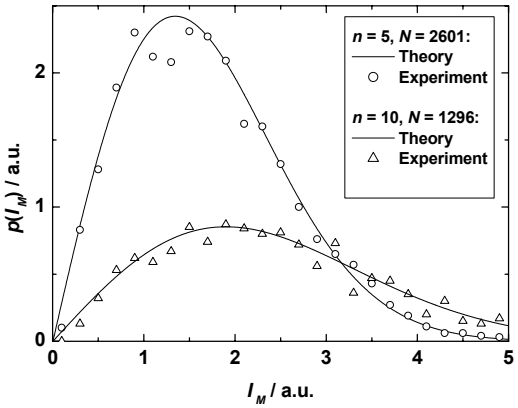

Fig. 2: $p(I_M)$ for $n = 5$ and $n = 10$

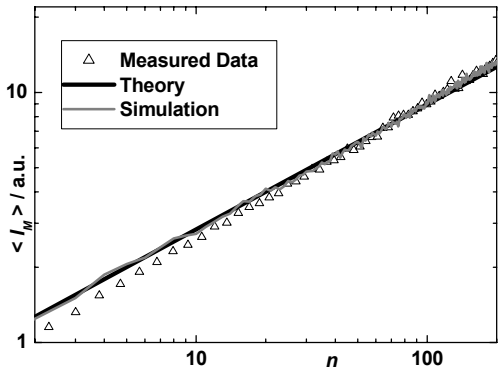

Fig. 3: $\langle I_M \rangle$ as function of speckle number n

4 Improvements of the ESPI-system with active phase stabilization

4.1 Digital PID-controller

In the new version of the phase stabilization system the analogue PID-controller was replaced by a digital one, which allows for a more simple adjustment of the P-, I-, and D-parameters and guarantees their exact reproducibility. This is particularly important if various variants of the control system shall be worked with (different modulation frequencies ω, change in control devices etc.). For the realization of the digital PID-controller a digital signal processor (DSP) of type Texas instrument C67EVM was used. The C67EVM is an *EV*aluation *M*odule, in which an AD/DA converter is integrated. These modules are used mainly in acoustical signal processing and their input and output stage have high-pass characteristics. This is useless

for the control system because the typical phase fluctuations lie in the frequency range under 50 Hz with a dominant contribution in the range under some Hz. Therefore the input and output stages were modified electronically so, that a nearly constant transfer function was achieved (Fig. 4).

The "old" control system with the analogue PID controller was operated at the following parameters: modulation frequency: $\omega/2\pi = 375$ Hz, modulation amplitude: $\alpha = 30°$ (resulting in $J_0(30°) = 0.93$; Eq. (4)), integration time of the LA: $\tau = 30$ ms, detector aperture: $D = 0.4$ mm, and speckle size: $d \approx 11$ µm. At first it was checked, whether the digital PID-controller reached an at least equal compensation of phase fluctuations at these parameters. For this measurement the object in the ESPI set-up (Fig. 1) was periodically deformed with a piezoelectric actuator, resulting in a triangle wave modulation of the phase Φ at the point P' with amplitude 27.5° and frequency f. The amplitude of the variation in the output signal of PD caused by this phase modulation was measured with a spectrum analyser with and without activated control system and from both quantities the damping was calculated. Fig. 5 shows that the damping using the digital controller is at least as good as the one achieved with the analogue controller. The dead time of the DSP (time delay between input and output signal) of 0.5 ms therefore doesn't affect the control behaviour in the interesting frequency range of phase fluctuations.

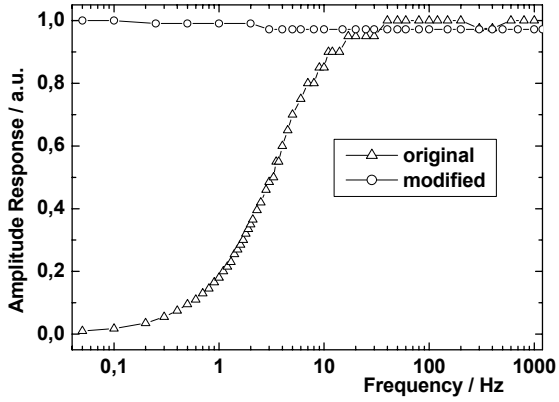

Fig. 4: Amplitude transfer function of the DSP

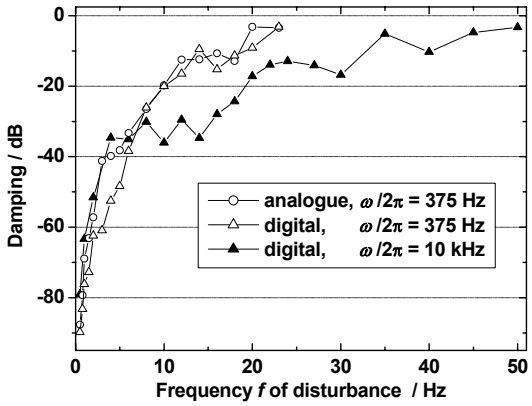

Fig. 5: Damping characteristic of the phase stabilization system

4.2 Increasing the cut-off frequency

In the next step the modulation frequency was increased to $\omega/2\pi = 10$ kHz. Thereby τ could be reduced from 30 ms to 1 ms, resulting in a higher cut-off frequency of the phase fluctuations $\varphi_g(t)$, which can be compensated for by the system. Fig. 5 shows that the damping in the frequency range above approx. 10 Hz could be improved significantly (notice the logarithmic scale). The fluctuations in the damping curves are caused by the global phase fluctuations $\varphi_g(t)$, which were present also during these measurements and influenced the experimental result in a random manner. In the future the modulation frequency shall be increased to 15 kHz, which is the highest frequency, at which the piezoelectric cylinder PZ_R still shows stable transient response. Thereby a further improvement of the damping is expected.

4.3 ESPI-measurements with unresolved speckles

As we have learned from Eq. (9), the expected value of the modulation, $\langle I_M \rangle$, in an integrated speckle interferogram increases with $\sqrt{n}$. From this point of view it is advisable to open not only the aperture A_{PD} of the photodetector PD but also the aperture A_{OB} of the objective, resulting in speckles that are no longer resolved by the pixels of the CCD camera. On the other hand, Eq. (8) states that at the same time the expected value of the background intensity, $\langle I_B \rangle$, increases with n so that the visibility V in an integrated interferogram recorded by the CCD-camera (Eq. (4)) decreases with $\sqrt{n}$. This is, however, insignificant if we consider ESPI subtraction images of two integrated interferograms 1 and 2 whose brightness B is proportional to:

$$(10) \qquad B \sim \left| \left\langle I_{1,\mathrm{CCD}} \right\rangle_t - \left\langle I_{2,\mathrm{CCD}} \right\rangle_t \right| = 2 I_M J_0(\alpha) \sqrt{\sin^2\left(\Theta_1 + \frac{\Delta\Theta}{2}\right)} \sqrt{\sin^2\left(\frac{\Delta\Theta}{2}\right)}$$

where we have assumed $I_{B,1} = I_{B,2}$, $I_{M,1} = I_{M,2}$, and $\Theta_2 = \Theta_1 + \Delta\Theta$. The fringe visibility V_B in this image is independent from the visibility V in the individual speckle interferograms and only limited by speckle decorrelation, which is unconsidered in Eq. (10). Therefore we expect the same fringe visibility V_B independent from the number n of speckles per pixel, as long as the object deformation (and therefore the speckle decorrelation) is the same and the modulation in the integrated speckle interferograms can be recorded with sufficient resolution, which requires a CCD-camera with high dynamic range. Fig. 6 shows an example confirming these results.

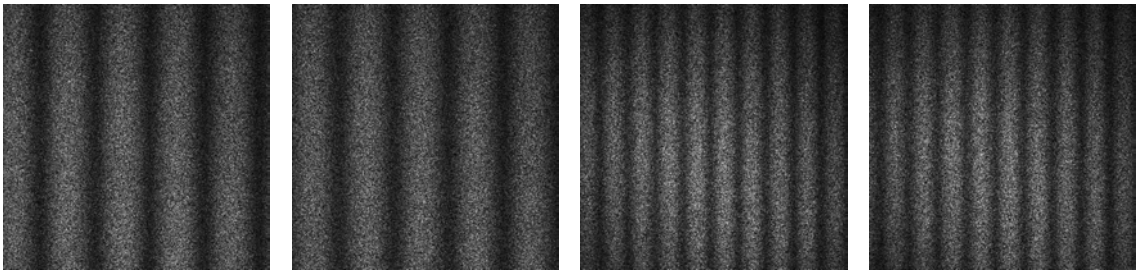

Fig. 6: ESPI subtraction images (Eq. (10)) with unresolved speckles. The interferograms $\langle I_{1,\mathrm{CCD}} \rangle_t$ and $\langle I_{2,\mathrm{CCD}} \rangle_t$ were recorded with a 12-Bit CCD-camera (Kodak ES 4.0). From left to right: $n \approx 3$, $V_B \approx 0{,}44$, $n \approx 6$, $V_B \approx 0{,}41$, $n \approx 23$, $V_B \approx 0{,}35$ $n \approx 56$, $V_B \approx 0{,}35$.

5 References

/1/ Creath, K.: Temporal Phase Measurement Methods, in: Robinson, D. W.; Reid, G. T. [Eds.]: *Interferogram Analysis*, Institute of Physics Publishing, Bristol, 1993, pp. 94-140

/2/ Burke, J.; Helmers, H.; Kunze, C.; Wilkens, V.: Speckle intensity and phase gradients: influence on fringe quality in spatial phase shifting ESPI-systems, Opt. Commun. 151.1-3 (1998) 144-152

/3/ Brozeit, A.; Burke, J.; Helmers, H.: Active phase stabilisation in electronic speckle pattern interferometry without additional optical components, Opt. Commun. 173.1-6 (2000) 95-100

/4/ Lehmann, M.: Phase-shifting speckle interferometry with unresolved speckles: A theoretical investigation, Opt. Commun. 128 (1996) 325-340

/5/ Goodman, J. W.: Statistical Properties of Laser Speckle Patterns, in: Dainty, J. C. [Ed.]: *Laser Speckle and Related Phenomena*, Springer, Berlin, 1975, pp. 9-75